Moth tails divert bat attack: Evolution of acoustic deflection

Jesse R. Barber[a,1], Brian C. Leavell[a], Adam L. Keener[a], Jesse W. Breinholt[b], Brad A. Chadwell[c], Christopher J. W. McClure[a,d], Geena M. Hill[b], and Akito Y. Kawahara[b,1]

[a]Department of Biological Sciences, Boise State University, Boise, ID 83725; [b]Florida Museum of Natural History, McGuire Center for Lepidoptera and Biodiversity, University of Florida, Gainesville, FL 32611; [c]Department of Anatomy and Neurobiology, Northeast Ohio Medical University, Rootstown, OH 44272; and [d]Peregrine Fund, Boise, ID 83709

Edited by May R. Berenbaum, University of Illinois at Urbana-Champaign, Urbana, IL, and approved January 28, 2015 (received for review November 15, 2014)

Adaptations to divert the attacks of visually guided predators have evolved repeatedly in animals. Using high-speed infrared videography, we show that luna moths (*Actias luna*) generate an acoustic diversion with spinning hindwing tails to deflect echolocating bat attacks away from their body and toward these nonessential appendages. We pit luna moths against big brown bats (*Eptesicus fuscus*) and demonstrate a survival advantage of ∼47% for moths with tails versus those that had their tails removed. The benefit of hindwing tails is equivalent to the advantage conferred to moths by bat-detecting ears. Moth tails lured bat attacks to these wing regions during 55% of interactions between bats and intact luna moths. We analyzed flight kinematics of moths with and without hindwing tails and suggest that tails have a minimal role in flight performance. Using a robust phylogeny, we find that long spatulate tails have independently evolved four times in saturniid moths, further supporting the selective advantage of this anti-bat strategy. Diversionary tactics are perhaps more common than appreciated in predator–prey interactions. Our finding suggests that focusing on the sensory ecologies of key predators will reveal such countermeasures in prey.

antipredator defense | bat–moth interactions | Lepidoptera | Saturniidae

Predators are under pressure to perform incapacitating initial strikes to thwart prey escape. It is thought that prey, in turn, have evolved conspicuous colors or markings to deflect predator attack to less vulnerable body regions (1, 2). Eyespots are a well-known class of proposed deflection marks (3), which are found in a variety of taxa, including Lepidoptera (3) and fishes (4), but only recently have experiments convincingly demonstrated that these color patterns redirect predatory assault. Eyespots on artificial butterfly (5) and fish (4) prey draw strikes of avian and fish predators. Eyespots on the wing margins of woodland brown butterflies (*Lopinga achine*) lure the attacks of blue tits (*Cyanistes caeruleus*) (6). Brightly colored lizard tails also divert avian predator attacks to this expendable body region (7).

Deflection coloration is unlikely to be an effective strategy against echolocating bats, as these predators have scotopic vision and poor visual acuity unsuited for prey localization and discrimination (8). Most bats rely on echoes from their sonar cries to image prey and other objects in their environment—they live in an auditory world (9). Thus, we would expect a deflection strategy, effective against bats, to present diversionary acoustic signatures to these hearing specialists. Weeks (10) proposed that saturniid hindwing tails might serve to divert bat attacks from essential body parts. We hypothesized that saturniid tails, spinning behind a flying moth (Movie S1) and reflecting sonar calls, serve as either a highly contrasting component of the primary echoic target or as an alternative target. We predicted that bats would aim their attacks at moth tails, instead of the wings or body, during a substantial percentage of interactions. To test this prediction, we pit eight big brown bats against luna moths with and without hindwing tails. To control for handling, we restrained each moth similarly and removed tails from approximately half of the individuals that were tested. Interactions took place under darkness in a sound-attenuated flight room. We recorded each engagement with infrared-sensitive high-speed cameras and ultrasonic microphones. To constrain the moths' flight to a ∼1 m^2 area surveyed by the high-speed cameras, we tethered luna moths from the ceiling with a monofilament line.

Results and Discussion

Bats captured 34.5% (number of moths presented; $n = 87$) of tailed luna moths, and 81.3% ($n = 75$) of moths without tails were caught—a 46.8% survival advantage for hindwing tails (Fig. 1). Mixed-effects logistic regression revealed a moth without tails is 8.7 times [confidence interval (CI) = 2.1–35.3] more likely to be captured than a moth with tails. During each foraging session, we presented a bat with one intact luna moth, one luna moth with its tails ablated, and 1–2 pyralid moths as controls. Control moths were captured 97.5% ($n = 136$) of the time. The adult big brown bats (*Eptesicus fuscus*) used in these experiments are not sympatric with tailed saturniid moths and are thus naive to this anti-bat strategy. Initial mixed-effects logistic regression analysis indicated that the number of nights bats hunted luna moths was not correlated with capture success ($P = 0.42$); bats did not learn to circumvent this defense over time. In addition, bats did not alter their sonar cries with experience or prey type (Fig. S1).

To determine if moths with intact tails lured bat attacks, we determined where on the moths' bodies the bats aimed their

Significance

Bats and moths have been engaged in acoustic warfare for more than 60 million y. Yet almost half of moth species lack bat-detecting ears and still face intense bat predation. We hypothesized that the long tails of one group of seemingly defenseless moths, saturniids, are an anti-bat strategy designed to divert bat attacks. Using high-speed infrared videography, we show that the spinning hindwing tails of luna moths lure echolocating bat attacks to these nonessential appendages in over half of bat–moth interactions. Further we show that long hindwing tails have independently evolved multiple times in saturniid moths. This finding expands our knowledge of antipredator deflection strategies, the limitations of bat sonar, and the extent of a long-standing evolutionary arms race.

Author contributions: J.R.B. and A.Y.K. designed research; J.R.B., B.C.L., A.L.K., J.W.B., G.M.H., and A.Y.K. performed research; J.R.B., B.C.L., A.L.K., J.W.B., B.A.C., C.J.W.M., G.M.H., and A.Y.K. analyzed data; and J.R.B. wrote the paper.

The authors declare no conflict of interest.

This article is a PNAS Direct Submission.

Data deposition: The data reported in this paper have been deposited in the Dryad Data Repository, datadryad.org (accession no. 0vn84).

[1]To whom correspondence may be addressed. Email: jessebarber@boisestate.edu or kawahara@flmnh.ufl.edu.

This article contains supporting information online at www.pnas.org/lookup/suppl/doi:10.1073/pnas.1421926112/-/DCSupplemental.

www.pnas.org/cgi/doi/10.1073/pnas.1421926112

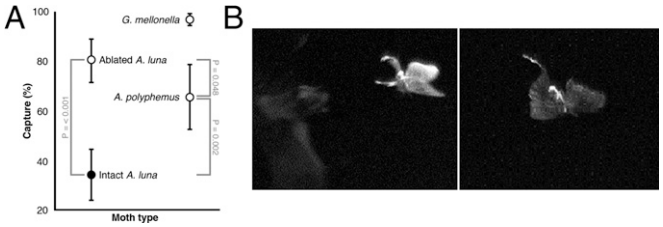

Fig. 1. Luna moth tails lure echolocating bat attacks. (*A*) Percentage of moths captured during interactions with big brown bats (*E. fuscus*). Error bars are binomial 95% CIs. Brackets show *P* values for comparisons using mixed-effects logistic regression. (*B*) Movie frames of a bat biting and removing the tail of a luna moth (*A. luna*).

strikes. We did so by reviewing three different high-speed camera angles of the interactions. Bats aimed at tails in 55.2% ($n = 87$) of interactions with intact moths (Movie S2), slightly more often than they aimed at the moth's body (44.8%, $n = 87$; binomial test, $P = 0.05$; Movie S3). Visual deflection marks are also usually found on the posterior of prey animals, which likely draws the predators' attack away from the escape trajectory (1–7). In fact, bats were rarely successful at capturing moths when they aimed at tails (4.2%, $n = 48$) but showed similar capture success to moths with tails removed when they targeted the body (71.8%, $n = 39$; binomial test, $P = 0.07$).

Bats often use an aerobatic capture technique that involves guiding the prey with a wing toward the midline of the bat before bringing the tail membrane toward the head where the insect can be bitten (Movie S4). In a more direct strategy, bats surround the prey with the wings and tail membrane concurrently and, in one motion, bring the insect to the mouth (Movie S3). When the bats in these experiments hunted intact luna moths, they generally approached from the side or behind the flying moth, using a direct strategy more often, biting and removing a tail (6.9%; Movie S5), damaging a tail (8.1%), or removing a section of hindwing near the tail (5.7%) in 20.7% ($n = 87$) of interactions. Once a moth was subdued, the bats in these experiments targeted the thorax first, likely to damage the moth's motor center and prevent it from escaping. Our data indicate that moth tails redirect these lethal attacks to expendable wing areas.

An alternative explanation of our results is that bats simply had a harder time capturing intact luna moths due to their greater wing size (11). To examine this possibility, we pit *Antheraea polyphemus* saturniid moths against the same bats, which are larger in area (body + wing, 71.6 cm^2) than intact luna moths (48.1 cm^2) yet lack tails. We found evidence that size does indeed provide a dividend: 66% ($n = 50$) of these moths were captured. However, this survival benefit compared with ablated luna moths does not explain the greater capture success of *A. polyphemus* compared with intact luna moths (Fig. 1; mixed-effects logistic regression, $P < 0.05$). Clearly, tails provide an anti-bat advantage beyond increased size alone. Enlarged and lobed hindwings might be functional intermediates on the way to the evolution of tails.

We cannot differentiate whether bats are targeting moth tails because they are a conspicuous element of a single target or are perceived as an alternative target. We might expect that information from multiple targets would increase attack latency (3), however using mixed-effects linear regression, we found no difference in latency between intact moths and those without tails ($t = -0.52$). Preliminary ensonification experiments indicate tails create distinct wing-like amplitude and frequency modulations on the returning echo stream of synthetic frequency-modulated (FM) signals (Fig. S2). Bats that use constant-frequency echolocation use the small amplitude and frequency modulations imposed on the returning echoes from beating insect wings to localize and discriminate prey (12, 13). However, only limited evidence indicates bats that emit FM sonar might do so, using information either within a single echo (14) or across an echo strobe group (15, 16). Regardless, the FM bats in these experiments were lured to the echoes of spinning tails.

To understand the historical pattern of tail evolution, we measured tail lengths of 113 saturniid moth species and constructed a phylogeny using maximum likelihood (ML) and Bayesian approaches. Trees from both analyses provided very similar results that are largely congruent (Fig. 2 and Fig. S3). Our results demonstrate four independent origins of long (>30 mm) hindwing tails with modified spatulate tips in the Saturniidae. Tails evolved in the well-supported *Actias* + *Argema* + *Graellsia* clade, *Copiopteryx*, *Eudaemonia*, and *Coscinocera*, which are placed in disparate tribes and two different saturniid subfamilies. Evidence for a single origin of tails is strongly rejected statistically (SH test, $P < 0.0001$). Examination of the tailed moth clades appears to show tail length increases from tailless or ancestrally shorter tails. Tail length might be increasing under selection from bats to move the echoic target created by spinning tails further from the body and forewings. Although a phylogenetic study with increased sampling focusing on these tailed clades is needed to support this conclusion, we note forewing damage in 8% ($n = 87$) of bat–luna moth interactions. It would be informative to look broadly across the Saturniidae and assess both the rates of damage to critical flight infrastructure (17) and bat capture rates of moths with longer (e.g., *Copiopteryx*, >100 mm) and shorter (e.g., *Arsenura*, <10 mm) tails than luna moths (average 37.5 mm).

Our data clearly support the anti-bat function of hindwing tails in luna moths, yet other selective forces might also be at work. Some saturniid moths are sexually dimorphic in wing morphology, including longer tails in males (18). However, it is difficult to separate sexual selection from the markedly different life history pressures on the sexes. Females often do not fly until mated and spend most of their short adult lifespan (average 4–8 d) disseminating pheromone from protected sites, dispersing short distances to oviposit (11). Male moths are the primary sex searching for mates and are under greater threat of bat predation (19). Saturniid moths are not known to use visual cues during mating, and the majority of species, including those with tails, are monoandrous, with females tending to mate with the first available male (20). Thus, it is unlikely that tails are used in mate choice. We view any possible influence of sexual selection on tails to be in addition to, not instead of, natural selection from bat predation.

Moth tails might also function in flight performance. To begin examining this possibility, we filmed luna moths flying in our flight room with ($n = 12$) and without ($n = 14$) hindwing tails with three synchronized, high-speed cameras. After handling the moths, we released them from one corner of the flight room and reconstructed their 3D escape flights. We calculated the mean values for wingbeat frequencies, speed, acceleration, normal acceleration (rate of direction change), normal acceleration in the horizontal plane (rate of direction change in the horizontal plane), and curvature (a measure of flight erraticism) over the flight period (Table S1). Due to highly correlated flight parameters ($r > 0.5$), we limited our analyses to speed, curvature, and wingbeat frequency. Logistic regression revealed that wingbeat frequency was the only parameter that significantly changed when hindwing tails were ablated ($P = 0.03$). The increase in wingbeat from 10 to 11 Hz in ablated moths likely indicates the moths were compensating for reduced lift or were less constrained by the reduced drag or mass from the removed hindwing area, but average kinematics involved in normal flight and predator evasion did not change.

More than half of the ~140,000 nocturnal moth species possess ears specialized to detect bat sonar (21). However, >65,000 species of nocturnal moths lack this acoustic defense (22) yet still face intense bat predation (23). Our data suggest that diversionary anti-bat defenses can be as successful as other acoustic strategies

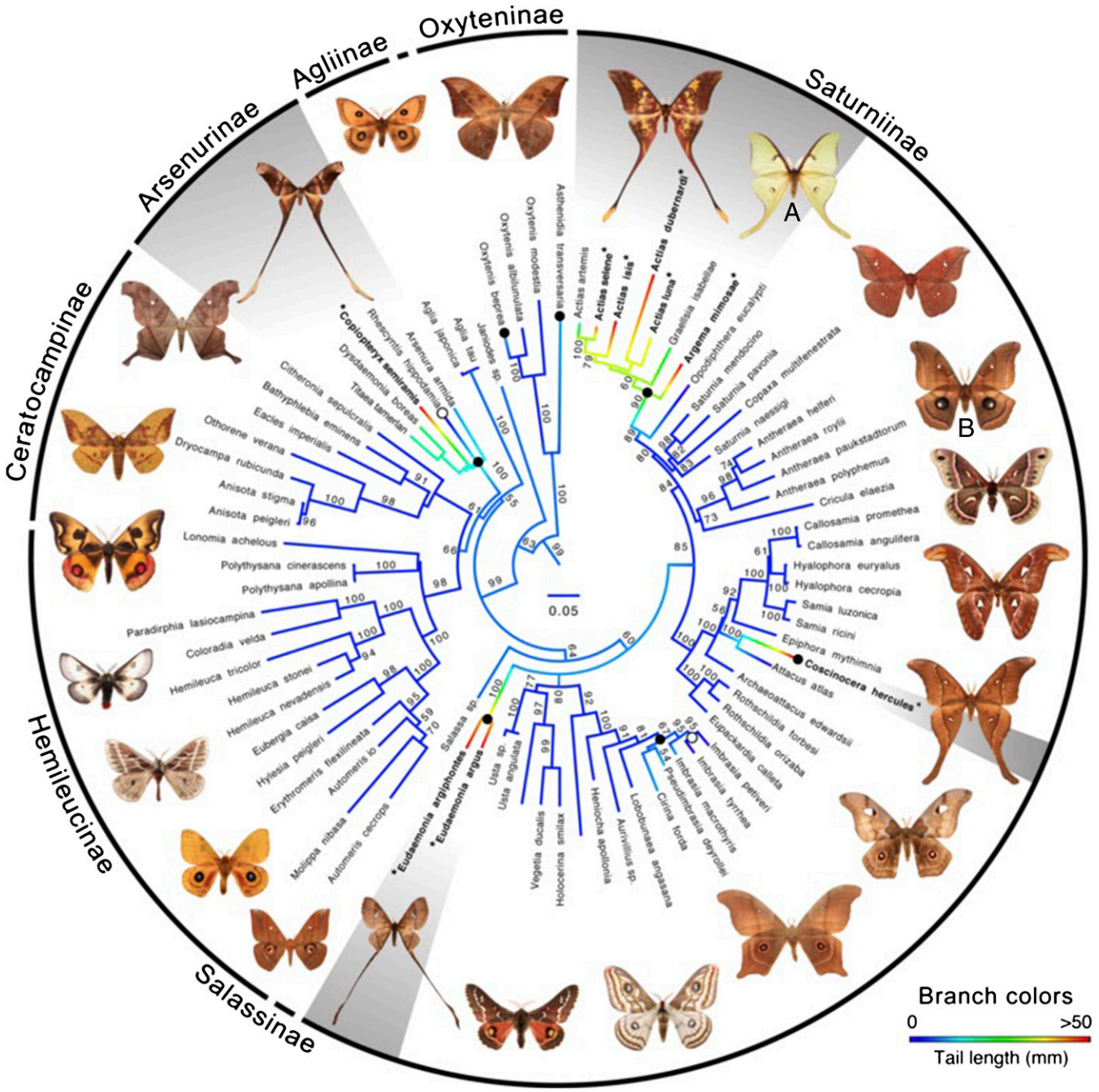

Fig. 2. ML molecular phylogeny of saturniid moths showing multiple independent origins of hindwing tails. Filled black circles indicate origin of tails. Open circles indicate losses. Branch colors indicate length of hindwing tail from absent (blue) to >50 mm (red), based on Phytools continuous character evolution analyses. Numbers by branches are bootstrap values. Gray shading denotes groups that have spatulate tails and contain species with tail lengths greater than 37.5 mm (the average for *A. luna*, $n = 10$). The images of saturniid moths used in these experiments are labeled: (A) *A. luna* and (B) *A. polypheumus*. Bold type and asterisks denote species that have tails longer than 37.5 mm. In combination with our bat–moth interaction data, this phylogeny suggests that tails serving a clear anti-bat function have evolved 4 times. Three additional origins of very short tails, of uncertain function, are also apparent.

in this arms race (24–26). Additional taxa with hindwing tails, including Lepidoptera and lacewings (27), might also be diverting predator attack to nonessential appendages. Our findings suggest that focusing on the sensory ecologies of important predators will reveal additional diversionary tactics in animals.

Materials and Methods

Animals. We mistnetted eight adult female big brown bats (*E. fuscus*) in Idaho and maintained them on a diet of mealworms (*Tenebrio* larvae) and moths used in experiments along with vitamin supplements. Recent molecular diet analyses reveal that *E. fuscus* consistently preys on Lepidoptera (28), making it a suitable model for these investigations. *Actias luna* and *A. polyphemus* moths were purchased from local providers as pupae, larvae, or eggs, or collected as adults (females only) in Gainesville, Florida, and placed into glassine envelopes where eggs were laid. We reared larvae in a temperature-controlled indoor laboratory at the Florida Museum of Natural History, McGuire Centre for Lepidoptera and Biodiversity (MGCL), in glass terrariums (30″ length × 12″ width × 12″ height) and fed them sweet gum (*Liquidambar styraciflua*) as their primary host plant. We used pyralid moths (*Galleria mellonella*), purchased as pupae from local providers, as positive controls in experiments.

Behavioral Experiments and Statistical Analysis. We conducted all vertebrate work with approval from Boise State University's Animal Care and Use Committee (IACUC 006-AC11-015) in a foam-lined indoor flight facility (7.6 m × 6.7 m × 3 m). We tethered moths to an 85-cm monofilament line through a small hole in the prothorax and visually compared the flight behavior of several moths tethered with this method to another approach that involved supergluing the line to the moth's prothorax. Because there were no differences in flight behavior, we used the former method to prevent the bats from ingesting glue. Eight bats hunted saturniid and control pyralid moths for 1–7 nights (average 3.75) each. We presented an approximate 70/30 ratio of male/female saturniid moths to bats; the species we used in these experiments are not sexually dimorphic in shape, but females are slightly larger in both species (18). To record each bat–moth interaction, we used three digital, high-speed, infrared-sensitive video cameras (Basler Scout, 120 frames per second) streaming to a desktop computer via a National Instruments PCIe-8235 GigE Vision frame grabber and custom LabView software. We illuminated the interaction space with eight infrared Wildlife Engineering LED arrays. To record echolocation, we mounted four ultrasonic condenser microphones [Avisoft CM16, ±3 dB(Z), 20–140 kHz] on the ceiling, in the four cardinal directions, 85 cm from the attachment point of the tether. XLR cables connected the microphones to a four-channel Avisoft UltraSoundGate 416H (sampling at 250 kHz) recording to a desktop computer running Avisoft Recorder software. We synchronized video and audio by triggering both with a National Instruments 9402 digital I/O module. We performed all statistical tests in R (29) and conducted mixed-effects regressions using the package lme4 (30). All mixed-effects regressions included the individual bats as random effects.

Echolocation Analysis. Using Avisoft SASLab Pro software, we analyzed the echolocation sequence of 2–4 attacks for each bat, 1–2 from attacks on intact luna moths and 1–2 from interactions with moths that had tails removed (total, 29). When possible, we chose a sonar recording from one of the first interactions between a naive bat and a luna moth and a second echolocation sequence from one of the last interactions we recorded, to examine learning effects. We selected a recording from one of four microphones to analyze based on signal-to-noise ratio. To calculate interpulse intervals (IPIs) of the sonar attack (31), we used the pulse train analysis tool. To limit potential off-axis effects between the bats' sonar and the microphones' directional sensitivity, we limited our spectral measurements to the frequency with minimum energy (F_{min}), a parameter less likely to be altered by varying recording conditions due to the decreased directionality of low frequencies. We calculated F_{min} as –15 dB from peak frequency using power spectra (Hann window, 1,024 fast fourier transform).

Ensonification Experiments and Analysis. To gain insight into the information luna moths provide to bats, we broadcast synthetic echolocation calls toward tethered flying moths and recorded the returning echoes. To fix the moth in place to standardize ensonification recordings, we first superglued a small rare-earth magnet to the top of a descaled portion of the thorax and then attached moths to a thin metal rod (Movie S1) with the long axis of their body fixed perpendicular to (90 degrees) and 40 cm from a speaker (Avisoft UltraSoundGate Player BL Pro-2, ±4 dB, 20–80 kHz) playing FM (70–30 kHz sweep, 2 ms pulse duration, IPI of 10 ms) synthetic echolocation signals. To prevent overlap between echoes from moths and the walls of our flight room, we were limited to an IPI of 10 ms for our playback stimuli. Big brown bats drop IPI to ∼6 ms during buzz II (31) and likely obtain more detailed wingbeat information from their prey than we visualize here (Fig. S2). Playbacks continued as long as the moth flew adeptly, up to 25 s. Echoes were recorded by a microphone (Avisoft CM16, ±3 dB, 20–140 kHz) adjacent to the speaker connected to an Avisoft UltraSoundGate 416H A/D sampling at 250 kHz onto a desktop computer running Avisoft Recorder software. We also filmed each trial with a Basler Scout high-speed camera at 100 frames per second that was synchronized with the audio recordings via a National Instruments 9402 digital I/O module that triggered both the video and audio. We ensonified luna moths under three conditions: (*i*) intact, (*ii*) tails removed, and (*iii*) wings occluded by sound-absorbing foam (serving as a "tails only" condition). In the last condition, Sonex foam was placed in front of the wings and body of the moth, leaving only the spinning tails "visible" to the microphone. In Avisoft SASLab Pro, we measured changes in relative peak amplitude imposed on the returning echoes using the pulse train analysis tool.

Flight Performance Analysis. We filmed both tailed and tailless luna moths during escape flights in our flight room with three synchronized, high-speed cameras (see *Behavioral Experiments and Statistical Analysis* for video equipment details). We calibrated our interaction space using a sparse bundle adjustment algorithm (32) implemented in custom MatLab software (33) that involves moving a "wand" of known dimensions through the interaction space. Next, we digitized each camera view and extracted 3D coordinates of moth flights. We applied a fourth-order, low-pass Butterworth filter with a 12-Hz cutoff frequency to reduce digitizing error. Fitting the filtered coordinates to a quintic spline function, we calculated the instantaneous measures of speed (magnitude of velocity), curvature (the turning rate of velocity, with respect to arc length, where a value of 0 represents a straight-line trajectory and increasing values indicate a sharper bending in the flight path), and linear acceleration (the rate of change in velocity over time) for the entire digitized moth flight using standard numerical analyses (34). We decomposed linear acceleration into two vectors: (*i*) normal acceleration, the component of acceleration due to the change of direction of the moth's flight path, and (*ii*) the horizontal normal acceleration, the component that occurs within the horizontal plane. To standardize the analyses of flights that varied in their duration, we calculated the mean values for all five variables during a 1-s flight period, beginning 20–50 frames after the moth was released to minimize the effects of the initial release on moth flight kinematics.

Calculating Average Body and Wing Area Size. We photographed six male specimens of *A. luna* and *A. polyphemus* from the MGCL collections. To image the moth on a white background, we pinned each specimen to a 3-mm opaque acrylic sheet and illuminated the area with two Yongnuo flashguns. We placed a reference scale near the specimens and photographed each individual at a consistent distance. We imported JPG files into ImageJ for analysis. A scale was set at 183.33 pixels/cm, and all images were changed to 8-bit. We measured the overlapping area of the forewing and hindwing on each side and added this value to the total area. The lower threshold was set between 220 and 240, and the upper threshold remained at 0. Depending on how the specimen was pinned, we measured the area of the head and antennae and subtracted that measurement from the total wing and body area size.

Saturniid Tail Measurements. We obtained specimens for tail measurements from the dried pinned collection of the MGCL. For each species, we measured up to 10 male specimens based on availability (113 species, 494 individuals) and tagged each specimen by placing a label with a unique identification number through the pin on the specimen. We prioritized measuring the right hindwing and took tail measurements where the margin of the wing began to offset away from the path of the wing margin. This point often occurred between wing veins (Fig. S4). We measured from the base of the wing to the tip of the tail. When a specimen lacked tails, we recorded the tail length as 0. For species that we could not obtain museum specimens, we examined digital images of adult specimens on the BOLD (www.boldsystems.org) database and quantified tail length with the scale in each image. For all specimens, we also measured the right forewing length (from where the Sc + R1 vein meets the base of the wing to the wing apex) with a digital caliper to correct for body size. When there was damage to the right wings, we chose the equivalent wing from the left pair. All wing measurements are included in Dataset S1.

Phylogenetic Methods. Using available nucleotide data from GenBank (35) and BOLD, we assembled data for five nuclear loci (*CAD*, *DDC*, *EF-1*, *Period*, and *Wingless*) and the COI mitochondrial gene for 80 taxa from Saturniidae and 34 taxa representing closely related bombycoid families, based on relationships inferred from recent deep phylogenetic studies of Bombycoidea (36–39). Individual loci were aligned with MAFFT v7.130b (40) and concatenated using Geneious 5.5.6 (www.geneious.com) and converted to the nexus format. We used PartitionFinder v1.1.1 (41) on the concatenated alignment to search for the best partitioning strategy and models among genes and codon positions using a greedy algorithm and the Bayesian information criterion (BIC) score (Dataset S1). Using RAxML 8.0.24 (42), we estimated phylogenetic trees with ML and ran Bayesian analyses with MrBayes 3.2 (43). We partitioned the dataset in RAxML following PartitionFinder results and applied the GTR+GAMMA model to all partitions and searched for the best tree with the "–f d" option using 200 random starting topologies and a combined bootstrap and likelihood search for 1,000 bootstrap pseudoreplicates with the "–f a" option following our previously published approach (44). For the Bayesian analysis, we followed the same partition scheme as used in RAxML but used PartitionFinder to optimize the models available in MrBayes. In MrBayes, we ran four independent Markov Chain Monte Carlo chains that consisted of one cold chain and three hot chains. Each run used default flat priors and was started from a random tree for 3×10^7 generations sampling every 1,000 generations. The variables

statefreq, revmat, shape, and pinvar were unlinked across all partitions, and models of evolution were set following PartitionFinder BIC results. To determine burn-in length, we made sure the average SD of split frequencies between runs fell below 0.01 and further used the program Tracer v1.5 (45) to check for convergence of the negative log likelihood values between chains. After deletion of burn-in, we combined MrBayes runs to make a majority-rule consensus tree with posterior probabilities.

Ancestral State Analysis and Statistical Tests of Tail Origins. We used the ML tree estimated in RAxML to conduct all ancestral state analyses. We first examined the number of origins of tails in Saturniidae with Mesquite 3.01 (46), using the Markov *k*-state 1 parameter model (MK1) (47). We then examined how tail length evolved on the tree, trimmed to saturniid taxa, using the continuous character mapping "contMap" in Phytools version 0.2–20 (48) that implemented the "fastAnc" function that computes ancestral states with Felsensteinen contrasts algorithm (49) for all internal nodes (Fig. S5). To correct for body size on phylogeny, we calculated the average ratio of tail length to body size (*Supporting Information*) and mapped these values on the ML tree with the contMap function in Phytools (Fig. S6). To test whether multiple origins of hindwing tails were more likely than a single origin, we conducted an SH test (50) on the ML topology in RAxML.

ACKNOWLEDGMENTS. We thank K. Miner, Z. Mroz, M. Eschenbrenner, and A. Acree for assistance with bat care and data analysis; G. Dewsbury, S. Epstein, D. Gluckman, D. Plotkin, and M. Standridge for assistance with moth rearing; J. McClung, E. Ortiz-Acevedo, P. Padrón, and P. Skelley for assistance with figures; R. Nuxoll and O. Bigelow for instrumentation support; E. Anderson for donating specimens; and W. Conner, M.-A. de Graaff, E. Hayden, P. Houlihan, D. Mennitt, K. Mitter, and D. Plotkin for comments and discussion. We acknowledge funding from National Science Foundation Grants IOS-1121807 (to J.R.B.) and IOS-1121739 (to A.Y.K.), postdoc support from the Florida Museum of Natural History (to J.W.B.), and undergraduate research support from the McNair Scholars Program (to A.L.K).

1. Poulton SEB (1890) *The Colours of Animals: Their Meaning and Use, Especially Considered in the Case of Insects* (D. Appleton, London).
2. Edmunds M (1974) *Defence in Animals* (Longman Group Limited, Essex, UK).
3. Stevens M (2005) The role of eyespots as anti-predator mechanisms, principally demonstrated in the Lepidoptera. *Biol Rev Camb Philos Soc* 80(4):573–588.
4. Kjernsmo K, Merilaita S (2013) Eyespots divert attacks by fish. *Proc R Soc B Biol Sci* 280(1766):20131458.
5. Vallin A, Dimitrova M, Kodandaramaiah U, Merilaita S (2011) Deflective effect and the effect of prey detectability on anti-predator function of eyespots. *Behav Ecol Sociobiol* 65(8):1629–1636.
6. Olofsson M, Vallin A, Jakobsson S, Wiklund C (2010) Marginal eyespots on butterfly wings deflect bird attacks under low light intensities with UV wavelengths. *PLoS ONE* 5(5):e10798.
7. Watson CM, Roelke CE, Pasichnyk PN, Cox CL (2012) The fitness consequences of the autotomous blue tail in lizards: An empirical test of predator response using clay models. *Zoology (Jena)* 115(5):339–344.
8. Eklöf J, Šuba J, Petersons G, Rydell J (2014) *Visual Acuity and Eye Size in Five European Bat Species in Relation to Foraging and Migration Strategies*. Available at eeb.lu.lv/EEB/201403/EEB_12_Eklof.pdf. Accessed November 15, 2014.
9. Ratcliffe JM (2010) Predator-prey interaction in an auditory world. *Cognitive Ecology II*, eds Dukas R, Ratcliffe JM (Univ Chicago Press, Chicago), pp 201–228.
10. Weeks AC (1903) Theory as to evolution of secondaries of moths of the genus catocala. *J NY Entomol Soc* 11(4):221–226.
11. Janzen DH (1984) Two ways to be a tropical big moth: Santa Rosa saturniids and sphingids. *Oxf Surv Evol Biol* 1:85–140.
12. Von der Emde G, Schnitzler H-U (1990) Classification of insects by echolocating greater horseshoe bats. *J Comp Physiol A Neuroethol Sens Neural Behav Physiol* 167(3):423–430.
13. Koselj K, Schnitzler H-U, Siemers BM (2011) Horseshoe bats make adaptive prey-selection decisions, informed by echo cues. *Proc R Soc B Biol Sci* 278(1721):3034–3041.
14. Grossetête A, Moss CF (1998) Target flutter rate discrimination by bats using frequency-modulated sonar sounds: Behavior and signal processing models. *J Acoust Soc Am* 103(4):2167–2176.
15. Kober R, Schnitzler H-U (1990) Information in sonar echoes of fluttering insects available for echolocating bats. *J Acoust Soc Am* 87(2):882–896.
16. Fontaine B, Peremans H (2011) Compressive sensing: A strategy for fluttering target discrimination employed by bats emitting broadband calls. *J Acoust Soc Am* 129(2): 1100–1110.
17. Jantzen B, Eisner T (2008) Hindwings are unnecessary for flight but essential for execution of normal evasive flight in Lepidoptera. *Proc Natl Acad Sci USA* 105(43): 16636–16640.
18. D' Abrera B (1995) *Saturniidae mundi=*. Available at agris.fao.org/agris-search/search.do?recordID=US201300022733. Accessed November 15, 2014.
19. Acharya L (1995) Sex-biased predation on moths by insectivorous bats. *Anim Behav* 49(6):1461–1468.
20. Morton ES (2009) The function of multiple mating by female Promethea moths, Callosamia promethea (Drury)(Lepidoptera: Saturniidae). *Am Midl Nat* 162(1):7–18.
21. Kristensen NP (2012) Molecular phylogenies, morphological homologies and the evolution of moth "ears." *Syst Entomol* 37(2):237–239.
22. Kristensen NP (1999) *Lepidoptera, Moths and Butterflies*. Available at agris.fao.org/agris-search/search.do?recordID=US201300091744. Accessed November 15, 2014.
23. Soutar AR, Fullard JH (2004) Nocturnal anti-predator adaptations in eared and earless Nearctic Lepidoptera. *Behav Ecol* 15(6):1016–1022.
24. Conner WE, Corcoran AJ (2012) Sound strategies: The 65-million-year-old battle between bats and insects. *Annu Rev Entomol* 57:21–39.
25. Kawahara AY, Barber JR (2015) Tempo and mode of anti-bat ultrasound production and sonar jamming in the diverse hawkmoth radiation. *Proc Natl Acad Sci USA*, 10.1073/pnas.1416679112.
26. Roeder KD (1974) Acoustic sensory responses and possible bat evasion tactics of certain moths. *Proceedings of the Canadian Society of Zoologists*, ed Burt MDB (University of New Brunswick Press, Fredericton, NB, Canada), pp 71–78.
27. Ylla J, Peigler RS, Kawahara AY (2005) Cladistic analysis of moon moths using morphology, molecules, and behaviour: Actias Leach, 1815; Argema Wallengren, 1858; Graellsia Grote, 1896 (Lepidoptera: Saturniidae). *SHILAP Rev Lepidopterol* 33(131): 299–317.
28. Clare EL (2014) Molecular detection of trophic interactions: Emerging trends, distinct advantages, significant considerations and conservation applications. *Evol Appl* 7(9): 1144–1157.
29. Team RC, et al. (2012) *R: A Language and Environment for Statistical Computing*. Available at cran.case.edu/web/packages/dplR/vignettes/timeseries-dplR.pdf. Accessed November 15, 2014.
30. Bates D, Maechler M, Bolker B, Walker S (2013) *lme4: Linear Mixed-Effects Models Using Eigen and S4. R Package Version 1.0-4*. Available at cran.r-project.org/web/packages/lme4/index.html. Accessed July 19, 2014.
31. Surlykke A, Moss CF (2000) Echolocation behavior of big brown bats, Eptesicus fuscus, in the field and the laboratory. *J Acoust Soc Am* 108(5 Pt 1):2419–2429.
32. Theriault DH, et al. (2014) A protocol and calibration method for accurate multi-camera field videography. *J Exp Biol* 217(Pt 11):1843–1848.
33. Hedrick TL (2008) Software techniques for two- and three-dimensional kinematic measurements of biological and biomimetic systems. *Bioinspir Biomim* 3(3):034001.
34. Crenshaw HC, Ciampaglio CN, McHenry M (2000) Analysis of the three-dimensional trajectories of organisms: Estimates of velocity, curvature and torsion from positional information. *J Exp Biol* 203(Pt 6):961–982.
35. Benson DA, Karsch-Mizrachi I, Lipman DJ, Ostell J, Wheeler DL (2005) GenBank. *Nucleic Acids Res* 33(Database issue, suppl 1):D34–D38.
36. Breinholt JW, Kawahara AY (2013) Phylotranscriptomics: Saturated third codon positions radically influence the estimation of trees based on next-gen data. *Genome Biol Evol* 5(11):2082–2092.
37. Zwick A (2008) Molecular phylogeny of Anthelidae and other bombycoid taxa (Lepidoptera: Bombycoidea). *Syst Entomol* 33(1):190–209.
38. Zwick A, Regier JC, Mitter C, Cummings MP (2011) Increased gene sampling yields robust support for higher-level clades within Bombycoidea (Lepidoptera). *Syst Entomol* 36(1):31–43.
39. Regier JC, Cook CP, Mitter C, Hussey A (2008) A phylogenetic study of the "bombycoid complex" (Lepidoptera) using five protein-coding nuclear genes, with comments on the problem of macrolepidopteran phylogeny. *Syst Entomol* 33(1):175–189.
40. Katoh K, Standley DM (2013) MAFFT multiple sequence alignment software version 7: Improvements in performance and usability. *Mol Biol Evol* 30(4):772–780.
41. Lanfear R, Calcott B, Ho SY, Guindon S (2012) Partitionfinder: Combined selection of partitioning schemes and substitution models for phylogenetic analyses. *Mol Biol Evol* 29(6):1695–1701.
42. Stamatakis A (2006) RAxML-VI-HPC: Maximum likelihood-based phylogenetic analyses with thousands of taxa and mixed models. *Bioinformatics* 22(21):2688–2690.
43. Ronquist F, et al. (2012) MrBayes 3.2: Efficient Bayesian phylogenetic inference and model choice across a large model space. *Syst Biol* 61(3):539–542.
44. Kawahara AY, et al. (2013) Evolution of Manduca sexta hornworms and relatives: Biogeographical analysis reveals an ancestral diversification in Central America. *Mol Phylogenet Evol* 68(3):381–386.
45. Rambaut A, Drummond AJ (2007) *Tracer v1. 4.* Available at beast.bio.ed.ac.uk/Tracer. Accessed January 1, 2014.
46. Maddison WP, Maddison DR (2014) *Mesquite: A Modular System for Evolutionary Analysis*, Version 3.01. Available at mesquiteproject.org. Accessed September 20, 2014.
47. Lewis PO (2001) A likelihood approach to estimating phylogeny from discrete morphological character data. *Syst Biol* 50(6):913–925.
48. Revell LJ (2012) phytools: An R package for phylogenetic comparative biology (and other things). *Methods Ecol Evol* 3(2):217–223.
49. Felsenstein J (1985) Phylogenies and the comparative method. *Am Nat* 125:1–15.
50. Shimodaira H, Hasegawa M (1999) Multiple comparisons of log-likelihoods with applications to phylogenetic inference. *Mol Biol Evol* 16:1114–1116.